



The power of simultaneous multi-frequency VLBI observations: Beyond frequency phase transfer

G. -Y. Zhao (KASI), J. C. Algaba, S. -S. Lee, T. Jung, R. Dodson, M. Rioja and the iMOGABA collaboration



1. Backgrounds

Atmospheric propagation effects

- Radio signals from the universe pass through the atmosphere and instruments before reaching to the detectors. All propagations bring errors to the data.
- At millimeter, it is mainly the **troposphere** which brings fast phase rotations. Such effects **can be well calibrated by Frequency phase transfer (FPT)** as they scale linearly with frequency (e.g. Jung et al. 2011, Rioja et al. 2015, Algaba et al. 2015).
- The **ionospheric effects**, however, **remain uncalibrated** after FPT. Moreover, these effects from the lower frequency are scaled up and brought to the higher frequency during FPT (e.g. Rioja & Dodson 2011).
- The **ionospheric effects also scale with frequency** (but different as tropospheric).

KVN and simultaneous multi-frequency receiving

- KVN can observe at up to 4 frequencies simultaneously.
- With KVN, we could have **>3 frequencies** \rightarrow **>2 FPT residuals**. So it is possible to also remove ionospheric effects by extending the conventional FPT.

2. Rationale: FPT-square

Raw visibility phases at different frequencies

structure	geometry	troposphere	ionosphere	instrument	thermal
ϕ_A^{v1}	$= \phi_{A, \text{str}}^{v1} + \phi_{A, \text{geo}}^{v1}$	$+ \phi_{A, \text{tro}}^{v1}$	$+ \phi_{A, \text{ion}}^{v1}$	$+ \phi_{A, \text{inst}}^{v1}$	$+ \phi_{A, \text{thermal}}^{v1} + 2\pi n_A^{v1}$
ϕ_A^{v2}	$= \phi_{A, \text{str}}^{v2} + \phi_{A, \text{geo}}^{v2}$	$+ \phi_{A, \text{tro}}^{v2}$	$+ \phi_{A, \text{ion}}^{v2}$	$+ \phi_{A, \text{inst}}^{v2}$	$+ \phi_{A, \text{thermal}}^{v2} + 2\pi n_A^{v2}$
ϕ_A^{v3}	$= \phi_{A, \text{str}}^{v3} + \phi_{A, \text{geo}}^{v3}$	$+ \phi_{A, \text{tro}}^{v3}$	$+ \phi_{A, \text{ion}}^{v3}$	$+ \phi_{A, \text{inst}}^{v3}$	$+ \phi_{A, \text{thermal}}^{v3} + 2\pi n_A^{v3}$

$\propto V$ Removed after FPT

Frequency phase transfer

R_{21}, R_{31} : frequency ratio

$\phi_{A, \text{FPT}}^{v2} = \phi_{A, \text{str}}^{v2} + 2\pi \bar{D}_{\lambda_2} \cdot \bar{\theta}_A^{v2} + \left(\frac{1}{R_{21}} - R_{21}\right) \phi_{A, \text{ion}}^{v1} + (\phi_{A, \text{inst}}^{v2} - R_{21} \cdot \phi_{A, \text{inst}}^{v1})$

$\phi_{A, \text{FPT}}^{v3} = \phi_{A, \text{str}}^{v3} + 2\pi \bar{D}_{\lambda_3} \cdot \bar{\theta}_A^{v3} + \left(\frac{1}{R_{31}} - R_{31}\right) \phi_{A, \text{ion}}^{v1} + (\phi_{A, \text{inst}}^{v3} - R_{31} \cdot \phi_{A, \text{inst}}^{v1})$

$\propto V^{-1}$ Still exist after FPT

Further step to remove the ionospheric effects: FPT-square

$\phi_{A, \text{FPT}^2}^{v3} = \phi_{A, \text{FPT}}^{v3} - R \cdot \phi_{A, \text{FPT}}^{v2}$ $R = \frac{(\frac{1}{R_{31}} - R_{31}) / (\frac{1}{R_{21}} - R_{21})}{\phi_{A, \text{ion}}^{v1}}$

$\rightarrow \phi_{A, \text{str}}^{v3} + 2\pi (\bar{D}_{\lambda_3} \cdot \bar{\theta}_A^{v3} - R \cdot \bar{D}_{\lambda_2} \cdot \bar{\theta}_A^{v2}) + [(\phi_{A, \text{inst}}^{v3} - R_{31} \cdot \phi_{A, \text{inst}}^{v1}) - R \cdot (\phi_{A, \text{inst}}^{v2} - R_{21} \cdot \phi_{A, \text{inst}}^{v1})]$

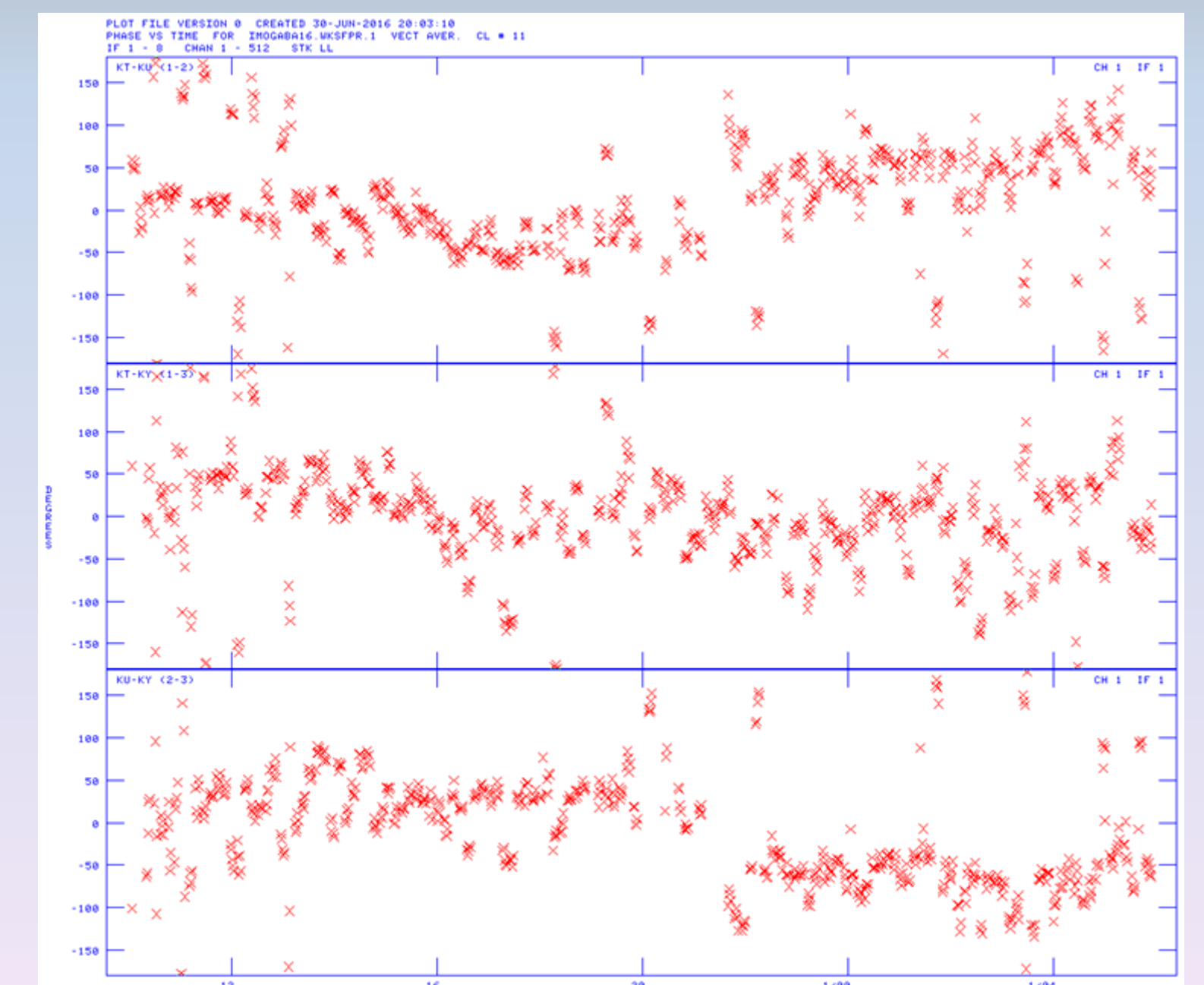
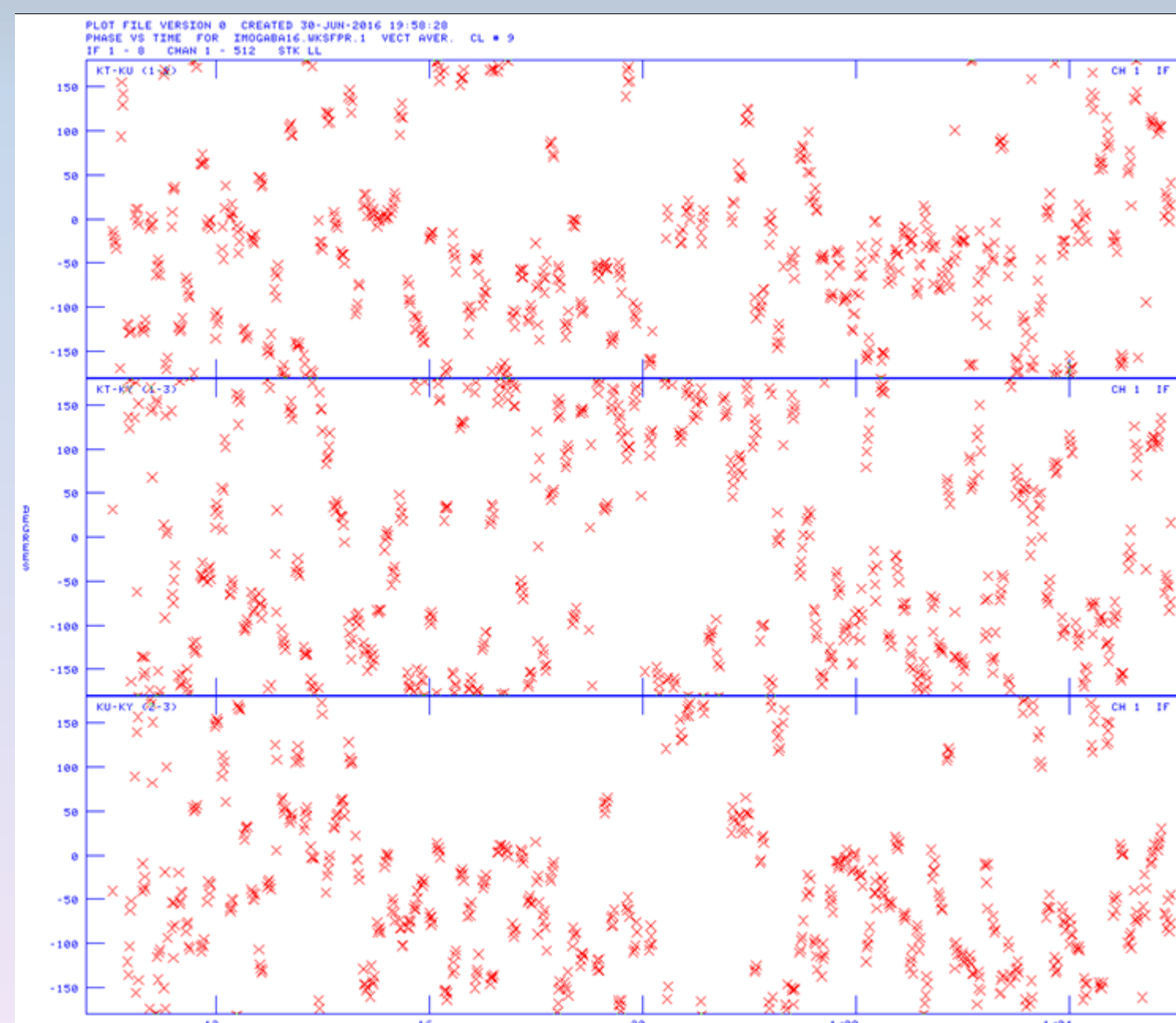
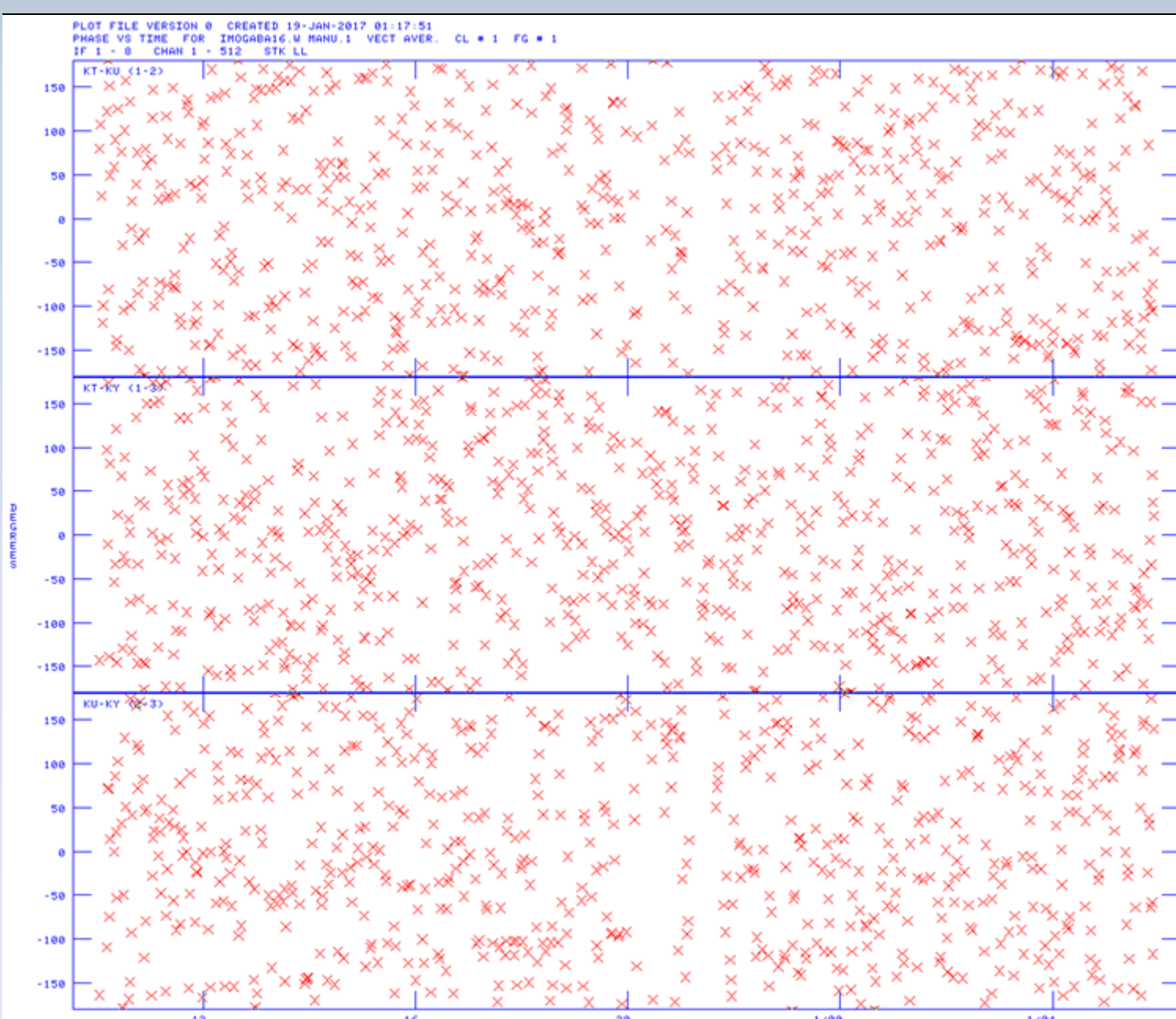
But can be removed in the same manner

Values of interest

Instrumental, Only thing left But slow, mostly stable

3. Application of FPT^2

- We tested the performance of KVN with FPT-square using an iMOGABA (Lee et al. 2016) observation, which is a ~20 hours session with 3 frequencies, 30 all-sky sources



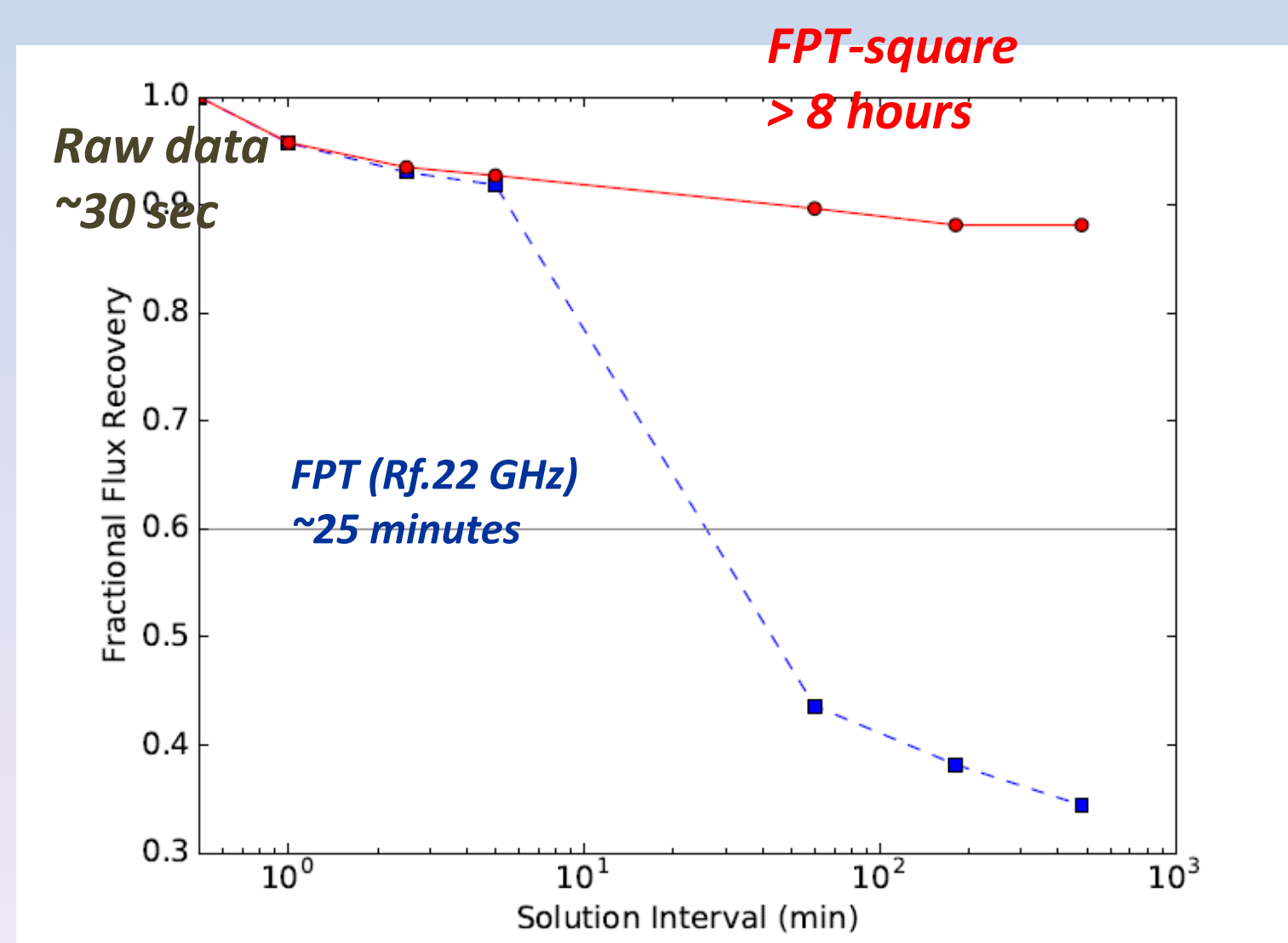
Raw phases at 86 GHz on each baseline. Tropospheric effects still exist, which cause fast phase rotations. The coherence time is short. This is also what we can get without simultaneous observing.

The phases on each baseline at 86 GHz after FPT from 22 GHz cm. Tropospheric effects are removed and phase coherence are improved. However, ionospheric effects start to dominate.

The phases on each baseline at 86 GHz after FPT^2 is applied: (FPT from 22 GHz, then FPT-square with 43 GHz FPT residual). Note this is a 20 hours long session with 30 different sources.

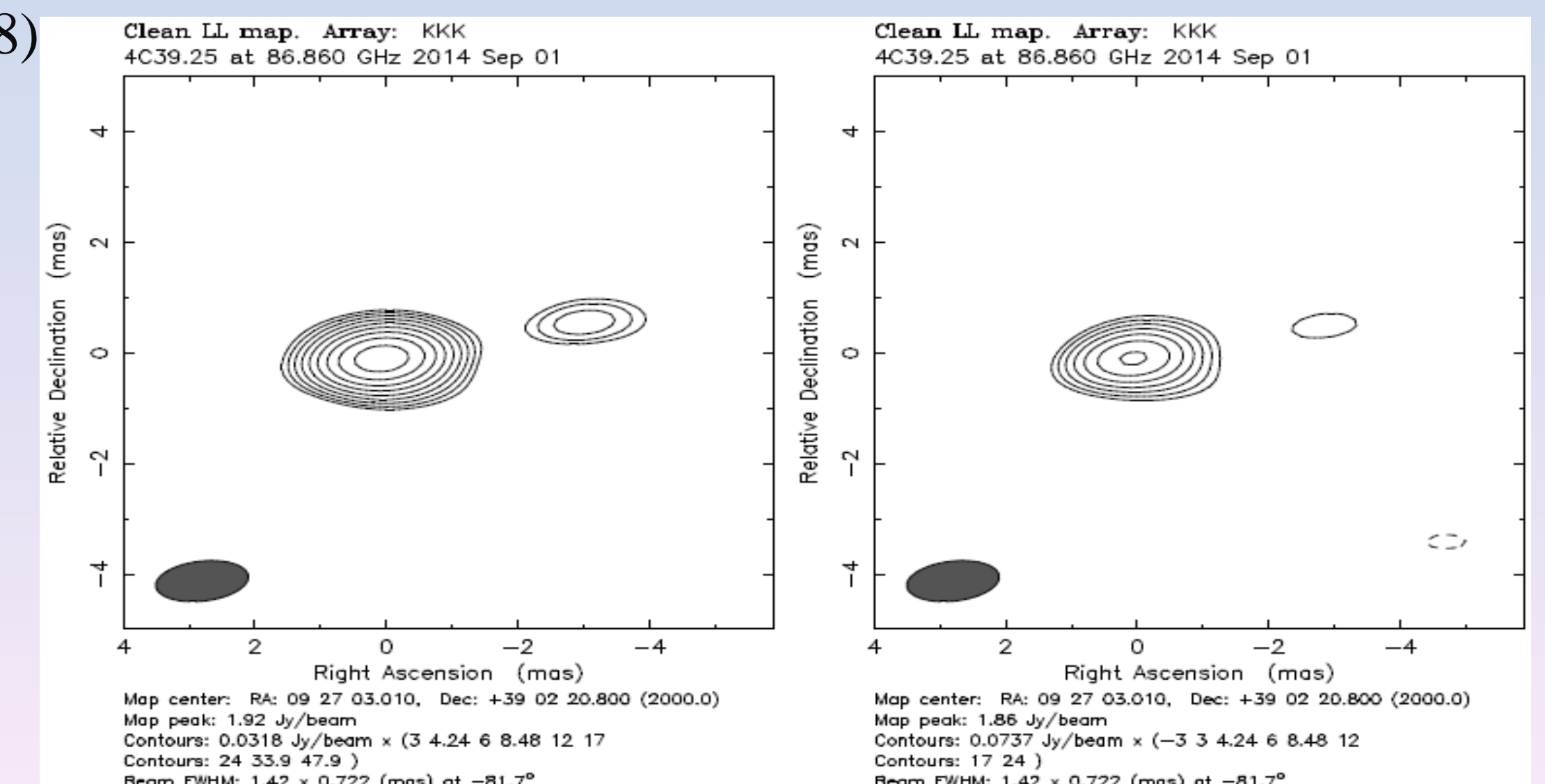
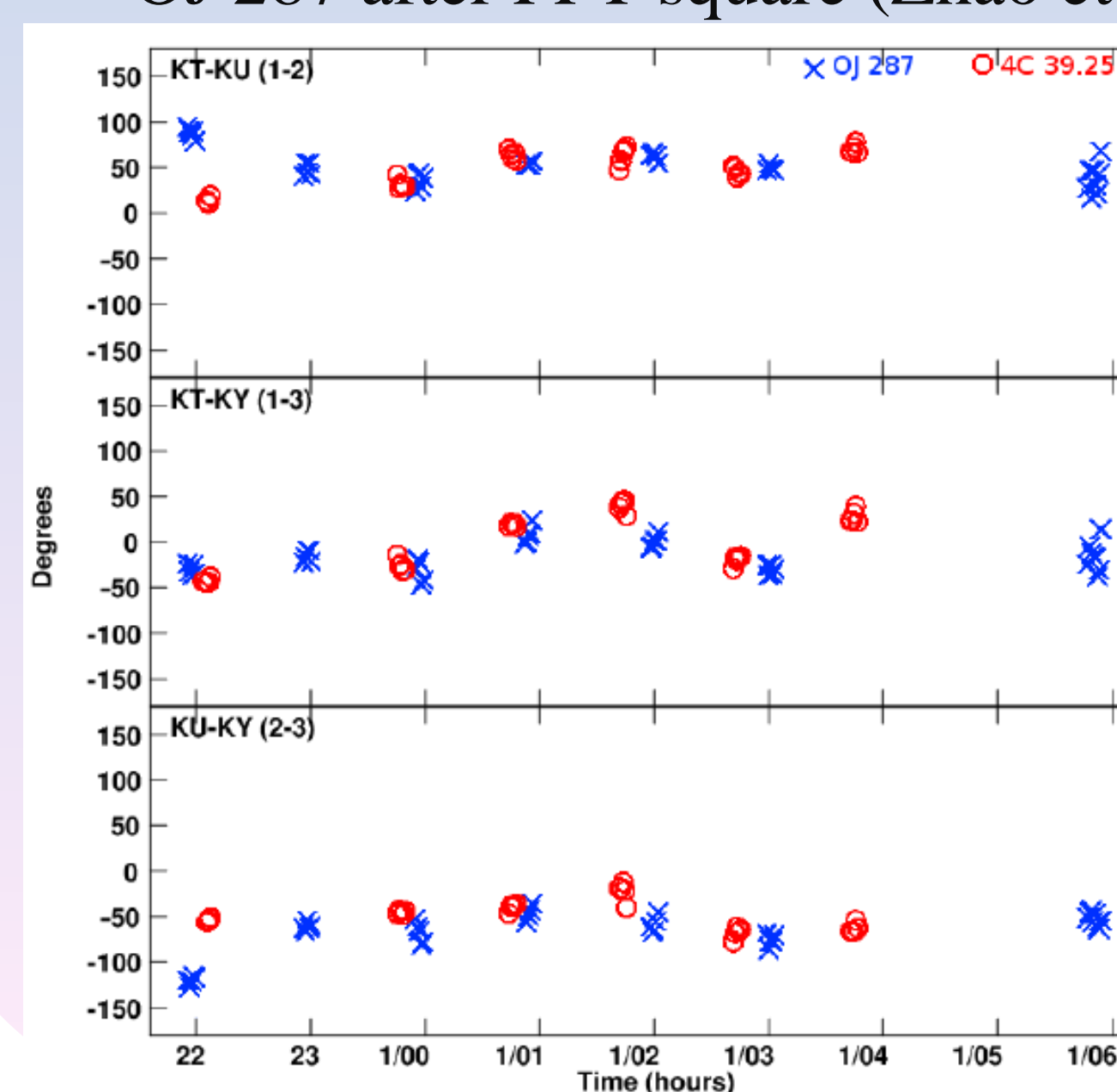
4. Increase of Coherence

- Fractional flux recovery at 86 GHz by fringe-fitting with different interval compared with the shortest.



5. Phase compensation between sources

- Residual phases after FPT-square also do not have significant line of sight dependence (Figures above). Phase solutions can be applied from one source to another **without tight constrains on source separation**.
- OJ 287 and 4C 39.25 are separated by ~20 degrees on the sky. But the FPT-squared phase are similar.
- We successfully detected the major structural components of 4C 39.25 by using the self-cal solutions of OJ 287 after FPT-square (Zhao et al. 2018)



The structure of 4C 39.25 at 86 GHz obtained by Left: self-calibration; Right: calibrated by OJ 287 after FPT-square

- One of the strength and uniqueness of FPT-square is the suitability for high frequency all sky surveys such as MASK (Jung's Poster).
- Note that a stable instrumental performance is very important for a successful FPT-square experiment. Implementation of a multi-frequency P-Cal system would be of great help.

References

- Algaba, J. C., Zhao, G.-Y., Lee, S.-S., et al., 2015, JKAS, 48, 257
 Jung, T., Sohn, B. W., Kobayashi, H., et al., 2011, PASJ, 63, 375
 Lee, S.-S., Wajima, K., Algaba, J.-C., et al. 2016, ApJ, 227, 8
 Rioja, M., & Dodson, R., 2011, AJ, 141, 114
 Rioja, M., Dodson, R., Jung, T., Sohn, B. W., 2015, AJ, 150, 202
 Zhao, G.-Y., Algaba, J.-C., Lee, S.-S. et al. 2018 AJ, 155, 26